



# Simplified energy-balance snowmelt modelling

*Thomas Skaugen and Tuomo Saloranta*

31  
2015

R  
A  
P  
P  
O  
R  
T



## **Simplified energy-balance snowmelt modelling**

**Utgitt av:** Norges vassdrags- og energidirektorat

**Redaktør:**

**Forfattere:** Thomas Skaugen and Tuomo Saloranta

**Trykk:** NVEs hustrykkeri

**Opplag:** 50

**Forsidefoto:** Heidi Bache Stranden/ NVE

**ISBN** 978-82-410-1078-1

**Sammendrag:** A first version of an energy balance (EB) based snow melt model is formulated, based on previous published work from several authors. The EB model uses only precipitation and air temperature as input, and the time-resolution is flexible (from hourly to daily). The algorithms of the EB model are presented in this technical research note, together with some evaluation results, where simulated and observed snow amounts and melt rates are compared. Comparison is also made between the EB-approach and the basic degree-day approach to snow melt modelling.

**Emneord:** Energy balance snowmelt model, Snow modelling

Norges vassdrags- og energidirektorat  
Middelthunsgate 29  
Postboks 5091 Majorstua  
0301 OSLO

Telefon: 22 95 95 95  
Telefaks: 22 95 90 00  
Internett: [www.nve.no](http://www.nve.no)

2015

# **Simplified energy-balance snowmelt modelling**

# Contents

<b>Preface .....</b>	<b>3</b>
<b>Summary.....</b>	<b>4</b>
<b>1 Introduction .....</b>	<b>5</b>
<b>2 The model.....</b>	<b>5</b>
2.1 Solar radiation.....	5
2.1.1 Solar radiation for $\Delta t$ less than daily.....	6
2.1.2 Alternative algorithm for the estimation of albedo.....	7
2.2 Long wave radiation.....	8
2.3 Turbulent fluxes - sensible and latent heats .....	9
2.4 Ground heat conduction.....	10
2.5 Precipitation heat .....	10
2.6 Cold content in snowpack .....	10
2.7 Iteration of snowpack- and snow surface temperatures.....	11
2.8 Structure of model.....	11
<b>3 Results .....</b>	<b>12</b>
3.1 Simulating accumulation and melt.....	12
3.2 Simulating snowmelt rates .....	19
<b>4 Discussion.....</b>	<b>22</b>
4.1 Simulating accumulation and melt.....	22
4.2 Simulating melt rates .....	25
4.3 Future prospects.....	25
<b>Conclusions.....</b>	<b>26</b>
<b>References .....</b>	<b>26</b>

# Preface

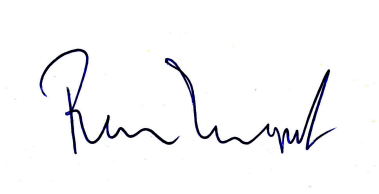
It has long, been an ambition to introduce energy balance (EB) modeling into the suite of snow models NVE. One reason is that it will enhance the competence and insight of the snow modelers at NVE, another is the fact that several studies have shown that at finer temporal resolutions than daily, an energy balance approach is superior to that of the degree-day approach used today. A third reason is that the input data available at some locations now comprises, wind speed and direction, short wave and long wave radiation, detailed temperature measurements at several horizontal layers etc. Also, Vormoor and Skaugen (2013) recently presented 3 hourly gridded (1 X 1 km) precipitation and temperature for all of Norway, with the objective of facilitating hydrological modeling (which necessarily includes snow modeling in Norway) at finer temporal resolution.

Oslo, April 2015

Morten Johnsrud  
Director

A handwritten signature in blue ink, reading 'Morten Johnsrud'.

Rune Engeset  
Head of Section

A handwritten signature in blue ink, reading 'Rune Engeset'.

# Summary

A first version of an energy balance (EB) based snow melt model is formulated, based on previous published work from several authors. The EB model uses only precipitation and air temperature as input, and the time-resolution is flexible (from hourly to daily). The algorithms of the EB model are presented in this technical research note, together with some evaluation results, where simulated and observed snow amounts and melt rates are compared. Comparison is also made between the EB-approach and the basic degree-day approach to snow melt modelling. Finally, some directions for future model development are outlined.

# 1 Introduction

In spite of examples of increased detail in meteorological data represented by, e.g. radiation and wind measurements, there is no indication that input data necessary for detailed energy balance (EB) modeling will be available for all of Norway at suitable temporal resolutions in the near future. Consequently, precipitation and temperature are the two meteorological input variables on which an EB approach to snow modeling have to be based. A possible gain in simulation results of snow accumulation and melt will hence be due to finer temporal resolutions of the said input. The limited meteorological information makes it necessary to use approximate relations to express quantities such as snowpack temperature, snow surface temperature, cloud cover, etc. as functions of precipitation and air temperature.

This study outlines an EB snow model where most of the governing equations are shamelessly copied from other authors with the aim of investigating the accuracy of an EB approach using only precipitation and air temperature as input.

## 2 The model

The daily energy budget of a column of snow is expressed as (Walter et al. 2005):

$$\lambda_F \rho_w \Delta SWE = S + L_a - L_t + H + LE + G + R - CC \quad (1)$$

and melt is estimated as:

$$\Delta SWE = (S + L_a - L_t + H + LE + G + R - CC) / (\lambda_F \rho_w)$$

where  $\lambda_F$  is the latent heat of fusion ( $\lambda_F = 335 \text{ kJ kg}^{-1}$ ),  $\rho_w [1000 \text{ kg m}^{-3}]$  is the density of water,  $\Delta SWE$  is the change in the snowpack's water equivalent [m],  $S [kJ m^{-2}]$  is the net incident solar (short wave) radiation,  $L_a [kJ m^{-2}]$  is the atmospheric long wave radiation,  $L_t [kJ m^{-2}]$  is the terrestrial long wave radiation,  $H [kJ m^{-2}]$  is the sensible heat exchange,  $LE [kJ m^{-2}]$  is the energy flux associated with the latent heats of vaporization and condensation at the surface,  $G [kJ m^{-2}]$  is ground heat conduction to the bottom of the snowpack,  $R [kJ m^{-2}]$  is heat added by precipitation and  $CC [kJ m^{-2}]$  is the change of snowpack heat storage. These fluxes are not routinely measured at a frequency and spatial coverage useful for operational national snow modeling, and the following will describe how these quantities are estimated as functions of location, time of year, precipitation and air temperature.

### 2.1 Solar radiation

The solar radiation striking a horizontal surface is:

$$S = S_0(1 - A)Y \sin(0.5\pi - \varpi) \quad (2)$$

where  $S_0 [kJ m^{-2} s^{-1}]$  is the potential solar radiation on a horizontal surface and readily estimated as:  $S_0 = \frac{1}{86400} 117.6 \times 10^3$ .  $A$  is the albedo and estimated for old snow

according to the empirical equation of US Army Corps of Engineers (1960) (Walter et al, 2005) as :

$$A = 0.35 - (0.35 - A_0)\exp(-(0.177 - \log(\frac{A_0-0.35}{A_{t-1}-0.35})^{2.16})^{0.46}) \quad (3)$$

Where  $A_0$  is the maximum albedo and assumed equal to  $A_0 = 0.95$  (Walter et al. 2005), and  $A_{t-1}$  is the albedo of the previous time step. It is, at present not known if eq. 3 is valid for temporal resolutions different from 24 hrs. In the case of new-fallen snow, the snow covers darker, old snow and Walter et al. (2005) suggested the following equation for estimating the albedo:

$$A = A_0 - (A_0 - A_{t-1})\exp(-\frac{4\Delta SWE\rho_0}{0.12}) \quad (4)$$

where  $\rho_0 [\text{kgm}^{-3}]$  is the density of new fallen snow and estimated as  $\rho_0 = 50 + 3.4(T_a + 15)$  where  $T_a$  is air temperature (Walter et al., 2005; after Goodison et al., 1981).

The variable  $Y$  is the net daily average sky transmissivity (Liston, 1995) and accounts for the scattering, absorption, and reflection of solar radiation:

$$Y = (0.6 + 0.2 \sin(0.5\pi - \varpi))(1.0 - 0.5Cl) \quad (5)$$

Here a discrepancy between Liston's papers (Liston, 1995; Pielke et al, 2004, Liston and Elder, 2006) and other authors is found. In Bacellar et al. 2008, the transmissivity is modeled as  $Y = 0.5 + 0.3 \cos \varpi$ , where  $\varpi$  is again the solar zenith angle. The expressions  $\sin(0.5\pi - \varpi)$  and  $\cos(\varpi)$  are interchangeable. The expression of Bacellar et al. (2008) is confirmed against observations and also provide good results in this study and is hence used in the following.

The variable  $Cl$  is the fractional cloudcover and estimated as zero if precipitation and 1 if not. The solar elevation angle  $\omega$  is defined as (Dingman, 2001):

$$\omega(t) = \arccos(\sin\varphi\sin\delta + \cos\varphi\cos\delta\cos(0.2618\tau)) \quad (6)$$

where  $\varphi$  is the latitude in radians,  $\delta$  is the solar declination angle in radians and equal to (Liston 1995):  $\delta = 0.4092\cos\left(\frac{2\pi}{365}\right)(DN - 173)$  ( $DN$  is the Gregorian day number) and  $\tau$  is the number of hours from solar noon, which gives  $\tau = 0$ . The variable  $\varpi$  used in Eq. 5, is the value of  $\omega$  averaged over the number of hours in each time step and is the solar zenith angle (Dingman, 2002), whereas the angle used in Liston (1995) is the solar elevation angle. These two angles are complementary to  $0.5\pi$ . (An algorithm coded in R transforming UTM (zone 33) coordinates to latitude and longitude is available from the authors).

### 2.1.1 Solar radiation for $\Delta t$ less than daily

In order to calculate the number of hours with solar radiation, the sunrise ( $S_r$ ) (hour) and sunset ( $S_s$ ) (hour) at the chosen location and day of year have to be determined. From algorithms found on the net we have:

$$S_r = (n - \Psi + Tz)/60 \quad (7)$$



and

$$S_s = (n + \Psi + Tz)/60 \quad (8)$$

where

$$n = 720 - 10 \sin\left(\frac{4\pi(DN-80)}{365.25}\right) + 8\sin\left(\frac{8\pi DN}{365.25}\right) \quad (9)$$

and

$$\Psi = \xi + 5 \quad (10)$$

where

$$\xi = 1440/(2\pi)\arccos\left(\frac{R-Z\sin\varphi}{F\cos\varphi}\right) \quad (11)$$

and where  $R$  is the radius of the earth,  $R = 6378$  [km],  $Z = r\sin\left(\left(\frac{2\pi}{365.25}\right)(DN - 80)\right)0.4092$ ,  $r$  is the distance to the sun  $r = 149598000$  [km], and  $F = (r^2 + Z^2)^{0.5}$ .

The time zone  $Tz$  is calculated as:  $Tz = -4(|\kappa| \bmod 15)\text{sign}(\kappa)$ , where  $\kappa$  is the longitude.

### 2.1.2 Alternative algorithm for the estimation of albedo

The “Utah Energy Balance Snow Accumulation and Melt Model” (UEB) (Tarboton and Luce, 1996) proposes an algorithm for estimating albedo as a function of snow surface age and solar illumination angle, which follows Dickinson et al. (1993).

Reflectance is computed for two bands, visible ( $< 0.7\mu m$ ) and near infrared ( $> 0.7\mu m$ ). The albedo,  $A$  is the average of the two reflectances:

$$\alpha_{vd} = (1 - C_v F_{age})\alpha_{v0}$$

$$\alpha_{ird} = (1 - C_{ir} F_{age})\alpha_{ir0}$$

Where  $\alpha_{vd}$  and  $\alpha_{ird}$  represent diffuse reflectances in the visible and near infrared bands. The constants  $C_v (= 0.2)$  and  $C_{ir} (= 0.5)$  quantify the sensitivity of the respective band albedo to snow surface aging (grain size growth) and  $\alpha_{v0} (= 0.85)$  and  $\alpha_{ir0} (= 0.65)$  are fresh snow reflectances in each band. The variable  $F_{age}$  accounts for the aging of the snow surface and is given by

$$F_{age} = \tau/(1 + \tau)$$

Where  $\tau$  is a non-dimensional snow surface age (starts as  $\tau=0$ , for fresh snow) that is incremented at each times step by the quantity designed to emulate the effect of the growth of surface grain sizes:

$$\Delta\tau = \frac{r_1 + r_2 + r_3}{\tau_0} \Delta t$$

Where  $\Delta t$  is the time step in seconds with  $\tau_0 = 10^6 s$ .

The parameter  $r_1$  depends on snow surface temperature ( $T_{ss}$  in °K here) intended to represent the effect of grain growth due to vapor diffusion:

$$r_1 = \exp(5000 \left( \frac{1}{273.16} - \frac{1}{T_{ss}} \right))$$

The parameter  $r_2$  represents the additional effect near and at freezing point due to melt and refreeze

$$r_2 = \min(r_1^{10}, 1)$$

and, finally,  $r_3 (= 0.03)$  represents the effect of dirt and soot.

A snowfall of  $P_s = 0.01 \text{ m}$  is assumed to restore the snow surface to new conditions ( $\tau=0$ ). With snowfall less than that in a time step, the dimensionless snow age is reduced by a factor  $(1-100P_s)$ .

The reflectance of radiation with illumination angle  $\varpi$  (the zenith angle of Dingman, 2001, measured relative to the surface normal) is computed as:

$$\alpha_v = \alpha_{vd} + 0.4f(\varpi)(1 - \alpha_{vd})$$

$$\alpha_{ir} = \alpha_{ird} + 0.4f(\varpi)(1 - \alpha_{ird})$$

Where

$$f(\varpi) = \frac{1}{b} \left[ \frac{b+1}{1+2b\cos(\varpi)} - 1 \right] \text{ for } \cos(\varpi) < 0.5$$

$$f(\varpi) = 0 \text{ otherwise}$$

The parameter  $b$  is set at 2 by Dickinson et al. (1993). The above equation increases reflectance for illumination angles larger than 60°.

When the snowpack is shallow, ( $SD < h = 0.1 \text{ m}$ ), the albedo is taken as

$$rA_{bg} + (1 - r)A$$

where  $r = \left(1 - \frac{SD}{h}\right) \exp\left(-\frac{SD}{2h}\right)$ , which interpolates between snow albedo and bare ground albedo ( $A_{bg}$ ) with the exponential term approximating the exponential extinction of radiation penetrating snow. The procedure for calculating albedo presented here (section 2.1.2) is the one used in the seNorge energy balance models, hereafter denoted *seNorge\_EB* model, although the other algorithms (US Army Corps of Engineers (1960) and Walter (2005) are coded and may be implemented.

## 2.2 Long wave radiation

The equations for atmospheric ( $L_a$ ) and terrestrial ( $L_t$ ) long wave radiation are adapted from Walter et al. (2005) and based on the Stefan- Boltzman equation:  $L = \varepsilon\sigma T_K^4$  where the Stefan-Boltzman constant is :

$$\sigma = 5,67 \times 10^{-11} \quad [kJm^{-2}K^{-4}s^{-1}]$$

An estimate of atmospheric emissivity is (Campbell and Norman, 1998):

$$\varepsilon_a = (0.72 + 0.005T_a)(1 - 0.84Cl) + 0.84Cl \quad (12)$$

where the fractional cloud cover  $Cl$  is estimated as in Eq. 5. The longwave atmospheric radiation is thus:

$$L_a = \varepsilon_a \sigma (T_a + 273.2)^4 \quad (13)$$

and estimating the emissivity of snow as a grey body, i.e.  $\varepsilon_s = 0.97$  the longwave terrestrial radiation is:

$$L_t = \varepsilon_s \sigma (T_{ss} + 273.2)^4 \quad (14)$$

Where  $T_{ss}$  is the snow surface temperature ( $^{\circ}C$ ).

## 2.3 Turbulent fluxes - sensible and latent heats

Sensible heat exchanges between surface and air is calculated with (Dingman, 2002, p. 197):

$$H = c_a \rho_a \frac{k^2}{(\log(\frac{z_{u,a}-d}{z_m}))^2} u \times (T_a - T_{ss}) \quad (15)$$

Where  $c_a$  is the heat capacity of air [ $kJ(kgK)^{-1}$ ],  $\rho_a$  is the density of air fixed at  $1.29 [kgm^{-3}]$ ,  $k = 0.41$  is von Karman's constant,  $z_u$  the height of the wind speed measurements and air temperature measurements ( $= 2 m$ ),  $z_m$  is the roughness height ( $= 0.001 m$ ),  $d$ , is the zero-plane displacement height ( $= 0 m$ ).  $\bar{T}$  is the average snowpack temperature (see subsection 2.6). This quantity changes sign dependent on the direction of the temperature gradient. Energy is lost if the snow is warmer than the atmosphere and  $H$  is negative.

Latent heat exchange between land surface and the atmosphere is governed by the same turbulent process as that of sensible heat exchange and is calculated from (Dingman, 2002):

If the snow surface temperature is less than zero ( $T_{ss} < 0$ ):

$$LE = (\lambda_V + \lambda_F) \times 0.622 \left( \frac{\rho_a}{Pa} \right) \times \frac{k^2}{(\log(\frac{z_{u,a}-d}{z_m}))^2} u \times (e_a - e_s) \quad [kJm^{-2}s^{-1}] \quad (16)$$

If the snow surface temperature is equal to zero ( $T_{ss} = 0$ ):

$$LE = \lambda_V \times 0.622 \left( \frac{\rho_a}{Pa} \right) \times \frac{k^2}{(\log(\frac{z_{u,a}-d}{z_m}))^2} u \times (e_a - e_s) \quad [kJm^{-2}s^{-1}] \quad (17)$$

Where  $\lambda_F$  and  $\lambda_V$  are the latent heats involved in fusion and vaporization-condensation respectively ( $\lambda_F = 335 kJkg^{-1}$ ,  $\lambda_V = 2470 kJkg^{-1}$ ),  $\rho_a$  is the density of air ( $\rho_a = 1.29 kg/m^3$ ),  $Pa$  is the air pressure ( $Pa = 101.1 kPa$ ), and  $e_a$  and  $e_s$  [ $kPa$ ] are

saturation vapor pressure in the atmosphere and at the surface respectively and can be estimated as (Dingman, 2002, p. 586, see also Walter et al. 2005)):

$$e_a = 0.611 \times \exp\left(\frac{17.3 \times T_a}{T_a + 237.3}\right) \quad (18)$$

and

$$e_s = 0.611 \times \exp\left(\frac{17.3 \times T_{ss}}{T_{ss} + 237.3}\right) \quad (19)$$

## 2.4 Ground heat conduction

Heat conduction from the ground to the snowpack is considered small and a constant in this model (from Walter et al. 2005 and the US Army Corps of Engineers (1960))

$$G = \frac{173}{86400} \quad [kJm^{-2}s^{-1}] \quad (20)$$

## 2.5 Precipitation heat

We assume rainwater has the same temperature as air and that heat is added to the snowpack when the rain's temperature is lowered to zero degrees:

$$R = \rho_w c_w P T_a \quad [kJm^{-2}] \quad (21)$$

Where  $c_w$  is the heat capacity of water ( $c_w = 4.19 [kJkg^{-1}K^{-1}]$ ) and  $P$  is rainfall [ $m$ ]

## 2.6 Cold content in snowpack

The change of heat storage in the snowpack is estimated as:

$$CC = \rho_w c_s SWE \times \bar{T} \quad (22)$$

Where  $c_s$  is the heat capacity of snow ( $c_s = 2.102 [kJkg^{-1}C^{-1}]$ ) and  $\bar{T}_N$  is an estimate of the snow pack temperature calculated as a weighted average of the air temperature for  $N$  days previous to current time step.  $\bar{T}_N$  is calculated as:

$$\bar{T}_N = \sum_{i=1}^N \lambda_i T_{a,i} \quad (23)$$

Where the weights  $\lambda$  are decreasing linearly with time, sum up to one, and are calculated as

$$\lambda_i = \frac{N-i+1}{N} \quad \sum \lambda_i = 1 \quad (24)$$

## 2.7 Iteration of snowpack- and snow surface temperatures

In winter, with cold conditions, the energy balance is very volatile. Sometimes, when temperatures of the snowpack is estimated to be much colder than the air temperature, we might have a transfer of energy to the snowpack that creates an energy surplus leading to melting, even when the temperature of both the snowpack and the air are below zero. This feature is remedied in the model with an adjustment of the snowpack (and snow surface-) temperature. If the model predicts melt ( $\Delta h_m$ ), the net energy change ( $S$ ) needed to produce the melt (Dingman, 2002, p.191) is :

$$S = -\frac{\Delta h_m \rho_w \lambda_f}{\Delta t} \quad (25)$$

The energy quantity  $S$ , can also be converted into a snowpack temperature change ( $\Delta \bar{T}$ ) (Dingman, 2002, p.191):

$$\Delta \bar{T} = \frac{\Delta t S}{c_s \rho_w SWE} = \frac{\Delta h_m \lambda_f}{SWE c_s} \quad (26)$$

The increase in snowpack temperature  $\Delta \bar{T}$  is added to the previously estimated snowpack temperature (Eq. 23), an adjusted snow surface temperature ( $T_{ss}$ ) is estimated ( $T_{ss} = 2\bar{T}$ ) and the energy balance (Eq. 1) is recalculated. This procedure reduces very efficiently the undesired melting events during cold conditions through decreasing the temperature difference between air and snowpack and hence changing the direction of the energy flow from the snowpack to the atmosphere. Note that this is a much simpler procedure than that used in e.g. Tarboton and Luce (1996) and avoids the use of tuning parameters.

## 2.8 Structure of model

Figure 1 shows the structure of the model. The alternative snowmelt modeling is implemented in the nedb\_eb subroutine of the seNorge R-model.

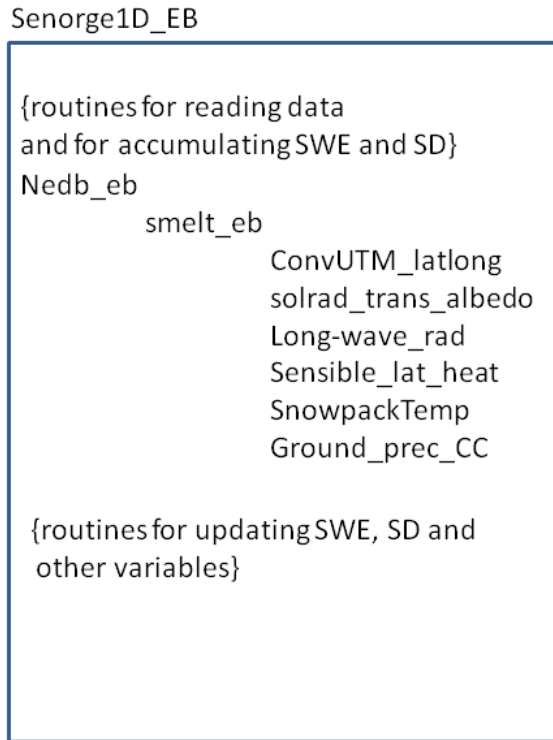


**Figure 1.** Structure of the *seNorge\_EB* model.

## 3 Results

### 3.1 Simulating accumulation and melt

The *seNorge\_EB* model was run as is, with input data (precipitation and temperature) from *seNorge* simulating SWE [mm], melt [mm], snow depth [cm], snow density and radiation elements without any calibration. All variables which are normally input to EB type models and which are not expressed as functions of precipitation and temperature are set as constants with values:

$u = 1.75$  Wind speed [m/s]

$Pa = 101.1$  Air pressure, [kPa]

Table 1 shows the Nash-Sutcliffe result for simulating SWE for 31 snow pillows. Figures 2-5 show examples of prognostic variable from the model. Figure 6 shows observed and simulated radiation (longwave and shortwave) and albedo at the Filefjell snow research site at 3 hourly resolution.

**Table 1.** Nash- Suthcliffe criterion (NS) for simulating SWE measured at 31 snowpillows. Bold letters signify the better model.”EB” denotes the *seNorge\_EB* model, “DG” the degree-day approach, and “SN” the operational seNorge model.

Snow station	NS_EB	NS_DG	NS_SN
2.36	<b>-1.75</b>	-2.22	-2.13
2.70	0.43	<b>0.48</b>	0.46
2.72	<b>0.67</b>	0.54	0.49
2.97	-5.93	<b>-5.81</b>	-6.50
2.373	0.91	<b>0.94</b>	<b>0.94</b>
2.382	<b>-1.36</b>	-2.0	-2.22
2.439	<b>-2.1</b>	-2.64	-2.87
2.451	<b>0.52</b>	0.46	0.33
8.5	<b>0.43</b>	0.41	0.33
12.142	<b>-0.37</b>	-0.72	-0.89
15.118	<b>-5.55</b>	-7.16	-7.85
16.232.14	<b>-5.1</b>	-5.55	-6.03
19.53	-18.11	<b>-13.91</b>	-16.95
19.78	<b>-0.27</b>	-0.51	-0.84
21.127	<b>-1.02</b>	-1.71	-2.20
26.67	<b>-3.69</b>	-3.93	-4.59
62.21	<b>-0.63</b>	-1.26	-1.59
73.11	<b>-3.35</b>	-3.97	-4.28
88.21	<b>-0.22</b>	-0.47	-0.67
121.2	-1.41	<b>-1.38</b>	-1.93
123.77	0.36	<b>0.37</b>	0.31
123.93	-0.42	-0.24	<b>-0.2</b>
139.4	0.75	<b>0.76</b>	0.68
156.63.3	<b>0.66</b>	0.49	0.36
164.120	<b>-0.97</b>	-1.32	-1.67

196.6	0.17	0.51	<b>0.56</b>
196.47.2	0.15	0.70	<b>0.77</b>
212.10	<b>0.56</b>	0.43	0.35
212.23	<b>0.65</b>	0.58	0.56
213.7	0.78	<b>0.91</b>	0.89
234.9	<b>0.60</b>	0.28	0.16



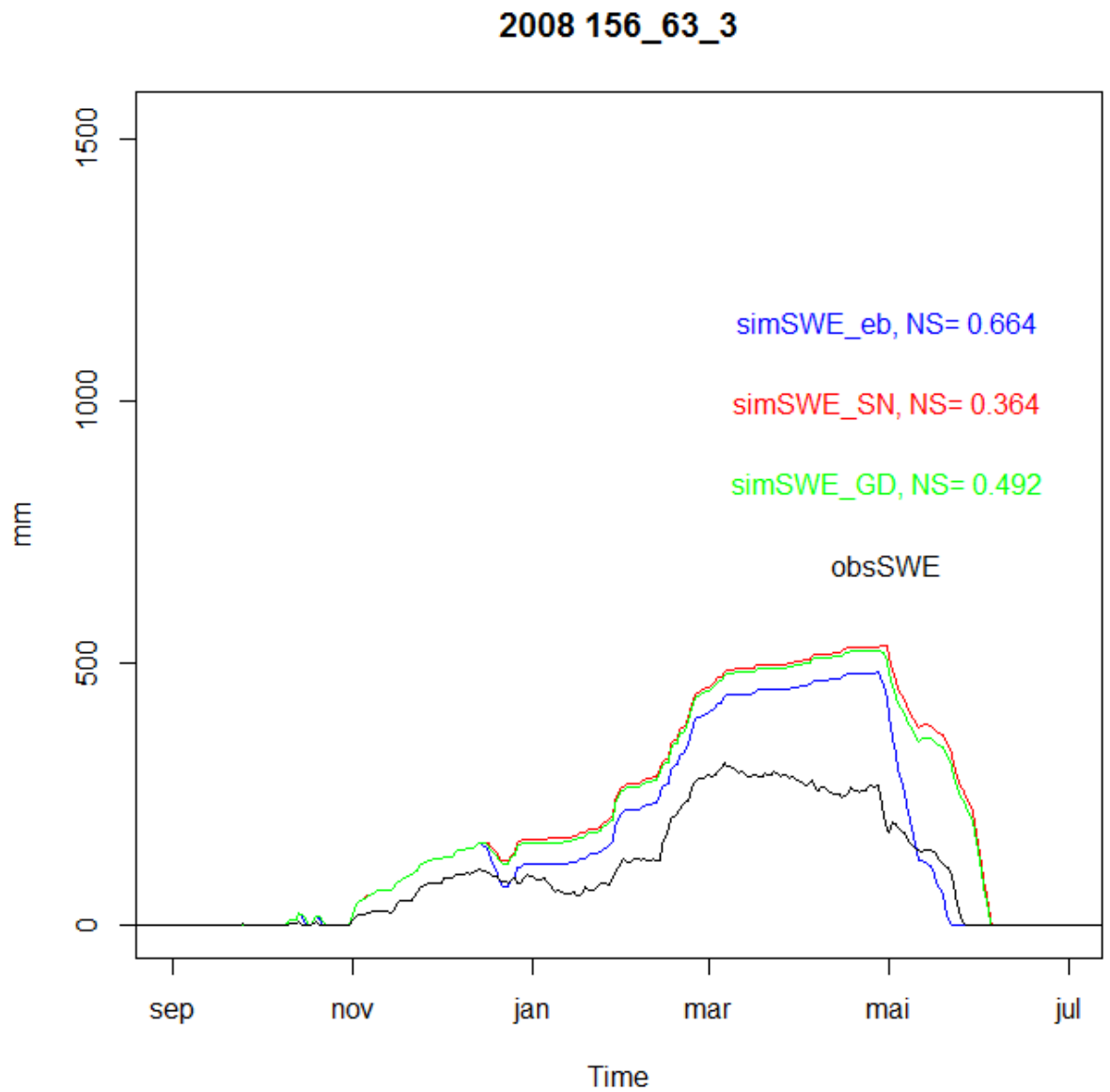


**Figure 2.** Simulated and observed SWE for the season 2007-8 for the station 156\_63\_3. Blue line is SWE simulated by the *seNorge\_EB* model, red line is the official *seNorge* SWE values for this site, and green line is SWE simulated by the *seNorge1D* using a degree-day approach.

2008 156\_63\_3

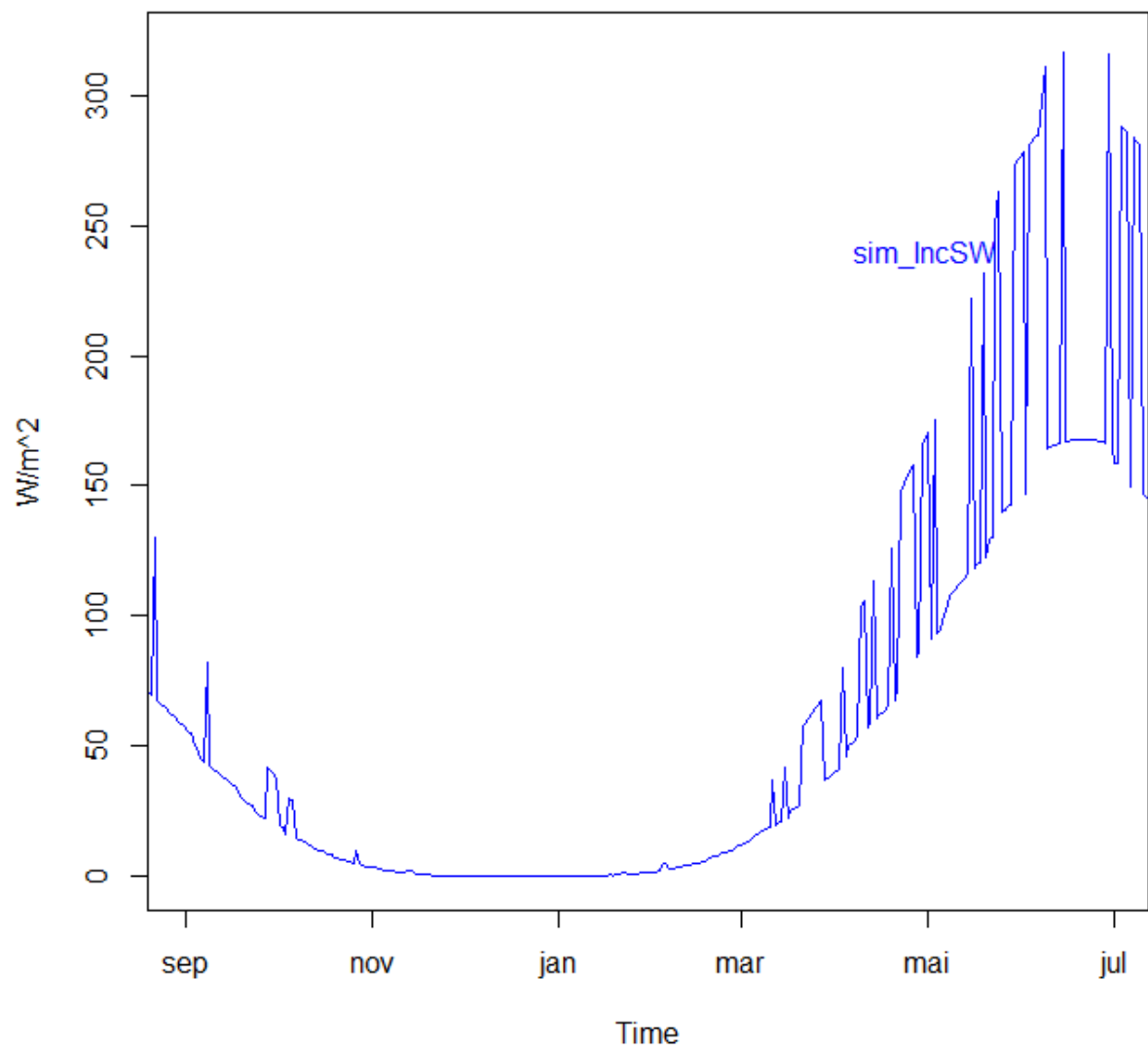


**Figure 3.** Simulated solar radiation for the season 2007-8 for the station 156\_63\_3.

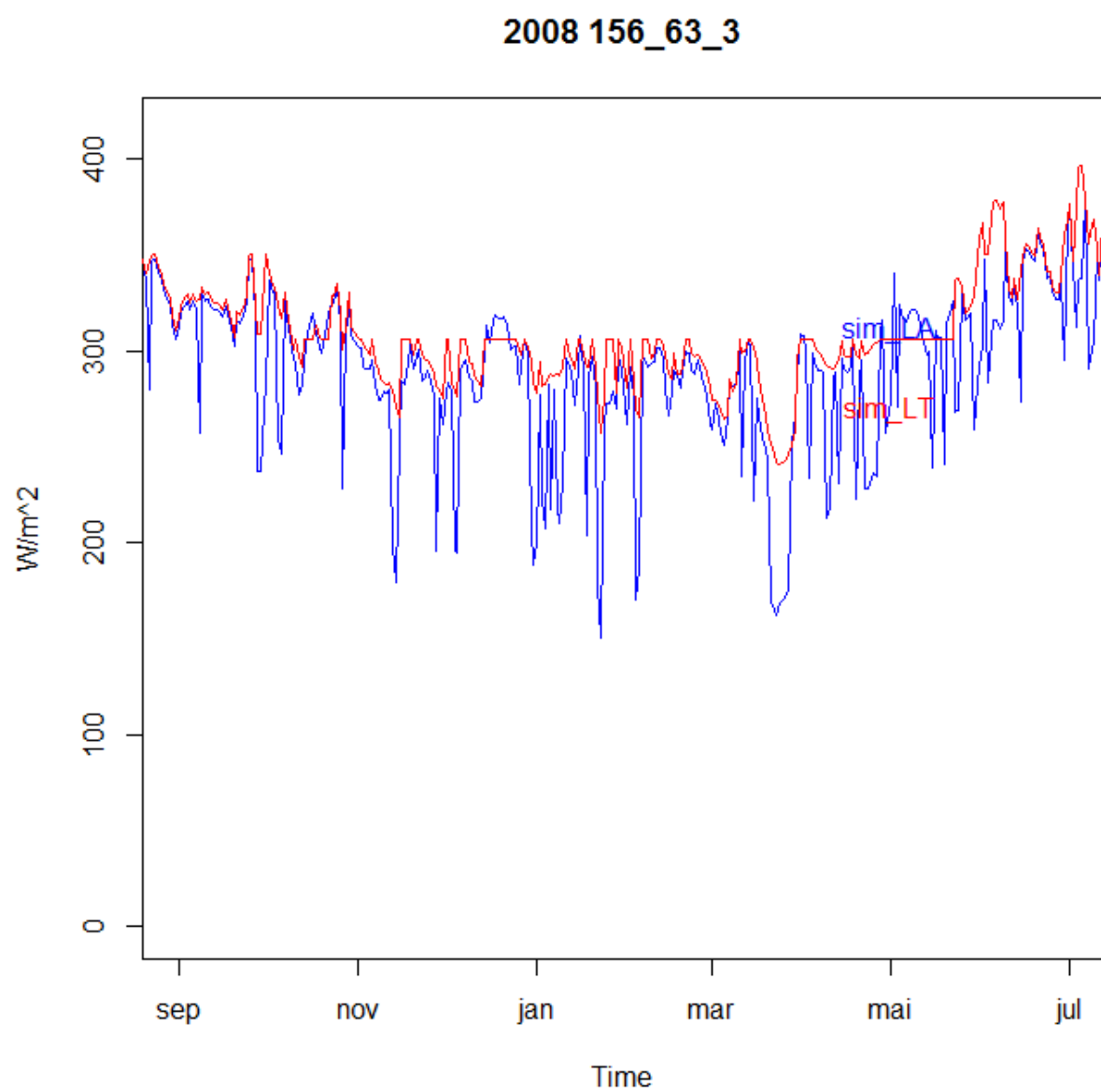


**Figure 4.** Simulated long wave terrestrial (red) and atmospheric (blue) radiation for the season 2007-8 for the station 156\_63\_3.

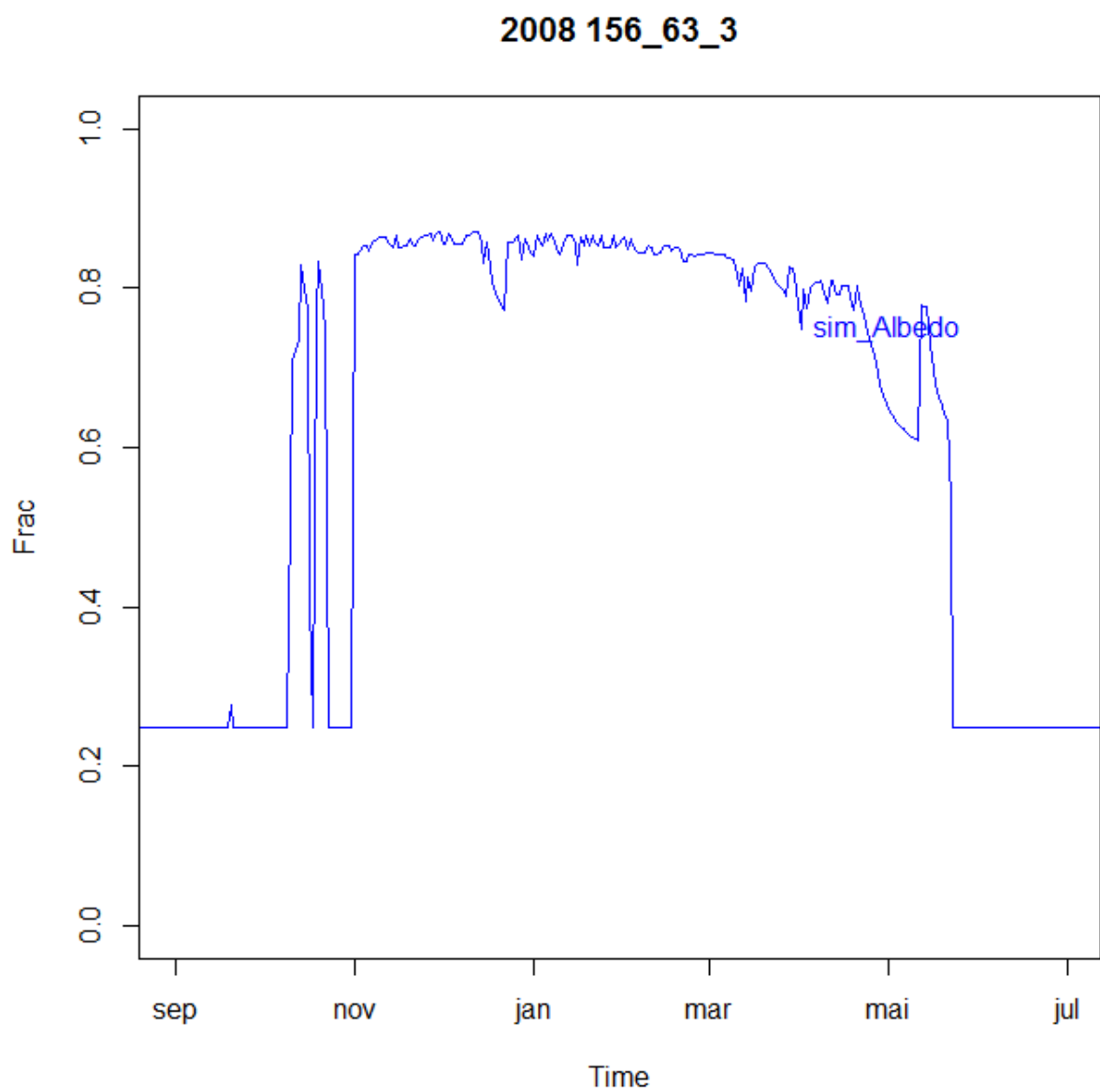


**Figure 5.** Simulated albedo for the season 2007-8 for the station 156\_63\_3 (UEB approach).

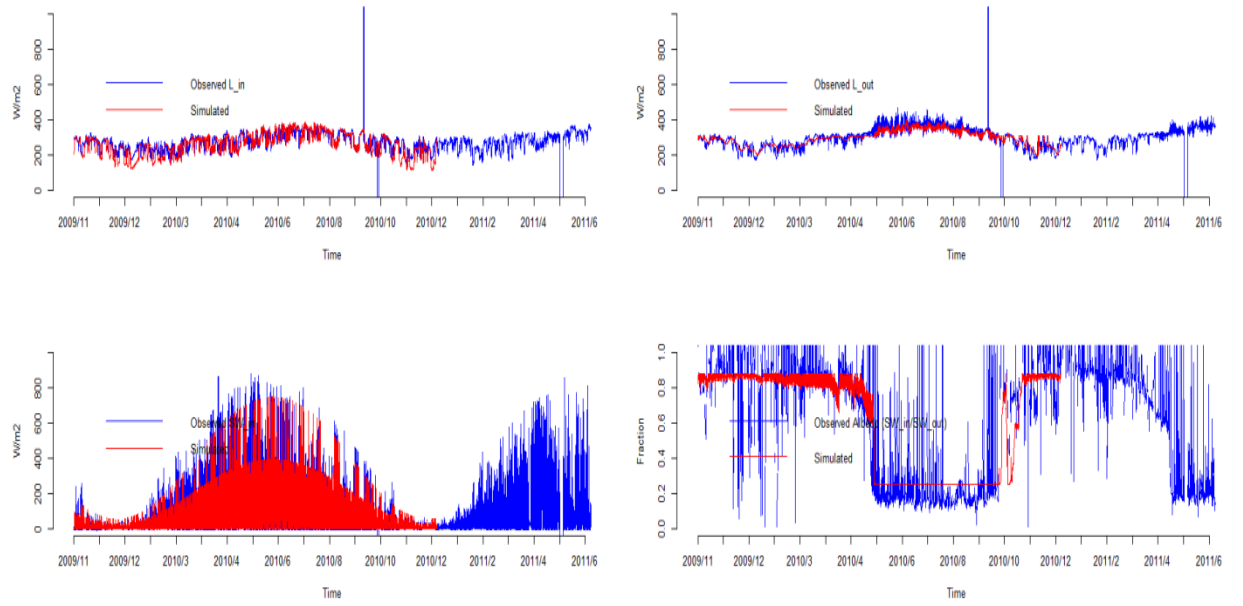


**Figure 6.** Simulated and observed atmospheric and terrestrial long wave radiation (top panels) short wave radiation (bottom left panel)- and albedo (bottom right panel) at Filefjell at temporal resolution of 3 hours. Input data (precipitation and temperature) are from the disaggregated gridded 3 hourly data set compiled by Vormoor and Skaugen (2013).

## 3.2 Simulating snowmelt rates

Simulated daily snow melt rates were tested against 3356 observations of daily snow melt rate from the NVE snow pillows (see Saloranta, 2014). The analysis was conducted via the R-script “*snowpillow.data.arrange.v2.R*” calling the snow melt module “*nedb\_eb.R*”. The melt simulations with *seNorge\_EB* were made in two steps:

**STEP 1:** The script “*nedb\_eb.R*” was first run daily over the period 1966-2011 for all 29 snow pillow stations, using the gridded temperature and precipitation, and simulated  $SWE_{ice}$  (assuming water-saturated snow and  $SWE_{ice} = 0.91 \cdot SWE$ ) from *seNorge.no* as input. The air temperatures of the last 5 days, as well as the value of the albedo parameter “*taux*” from previous time step, were saved each day.

**STEP 2:** Then, a new round of simulations was conducted for the 3356 snow melt rate observations from different dates and snow pillow stations. The simulation setting was similar to STEP 1 described above, except that now the observed  $SWE$  (converted to  $SWE_{ice}$  as above) at snow pillow station and the previously saved albedo parameter “*taux*” from STEP 1 were used as input. The simulated snow melt rates ranged from  $-3$  to  $64$  mm/d (negative values indicate potential refreezing of liquid water in the snow pack).

The results indicate that the *seNorge\_EB* snow melt model simulates the variability of snow melt rates roughly as good as the degree-day based model *seNorge v.1.1.1*, but that

it has a significant positive bias in simulating the observed snow melt rates (Table 2; Figures 7-8). This bias increases with temperature and along the snow melt season (Figure 8; temperature, of course, also increases along the snow melt season). Note that the current seNorge snow model version v.1.1.1 includes a revised melt algorithm where a solar radiation-dependent term is added to the basic degree-day equation (Saloranta, 2014). The two parameters of this revised melt model are calibrated using the melt rate data from the snow pillows.

**Table 2.** Melt model fit statistics for the forest and treeless subsets of snow pillow data, using the previous (v.1.1) and current (v.1.1.1) version of the seNorge melt model, as well as the energy balance approach (*seNorge\_EB*).

<b>Treeless subset</b>	<b>R<sup>2</sup></b>	<b>NS</b>	<b>median bias</b>	<b>% bias of melt sum</b>
<i>seNorge v.1.1</i>	?	0.03	?	–13 %
<i>seNorge v.1.1.1</i>	0.20	0.20	+1 mm/d	no bias
<i>seNorge_EB</i>	0.21	-1.0	+8 mm/d	+43 %

<b>Forest subset</b>	<b>R<sup>2</sup></b>	<b>NS</b>	<b>median bias</b>	<b>% bias of melt sum</b>
<i>seNorge v.1.1</i>	?	0.31	?	–7 %
<i>seNorge v.1.1.1</i>	0.35	0.35	+1 mm/d	no bias
<i>seNorge_EB</i>	0.29	-2.2	+12 mm/d	+76 %

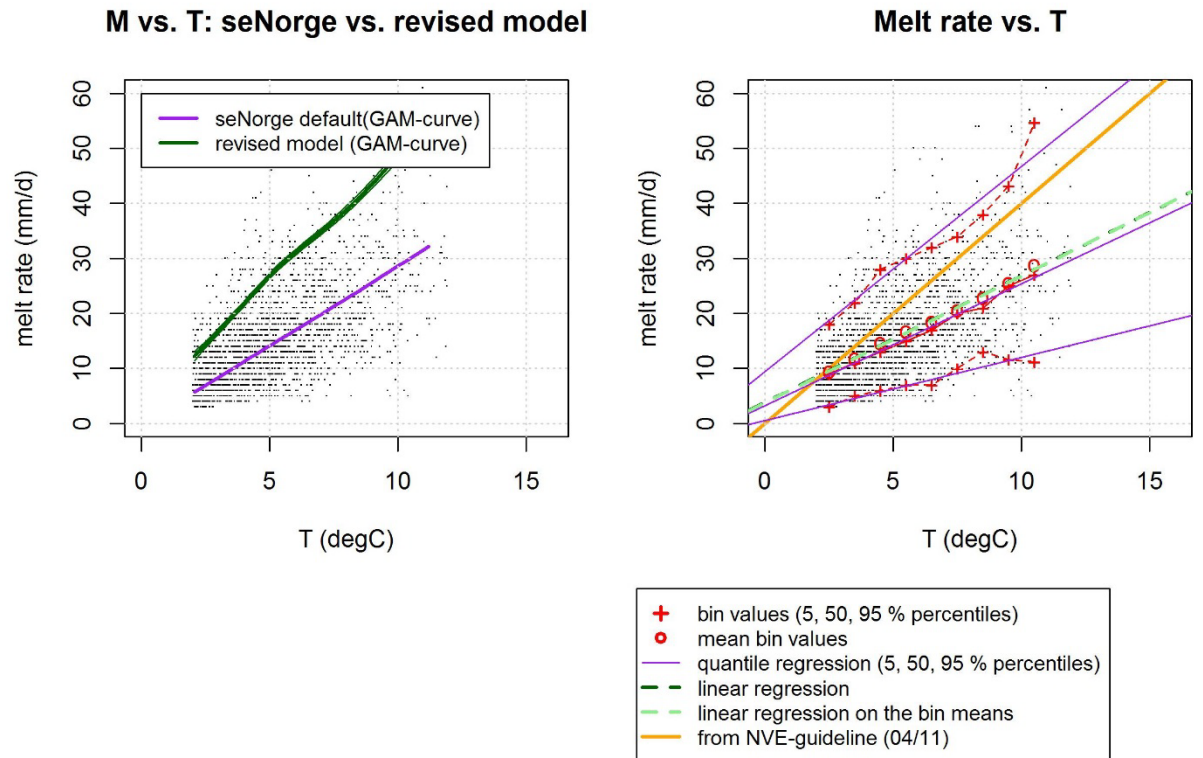


**Figure 7.** Different melt models' fit for the forest subset of snow pillow data. Green line in the left panel denotes the *seNorge\_EB* model. Orange and blue lines denote the *seNorge\_EB* and the *seNorge v.1.1.1* models respectively.

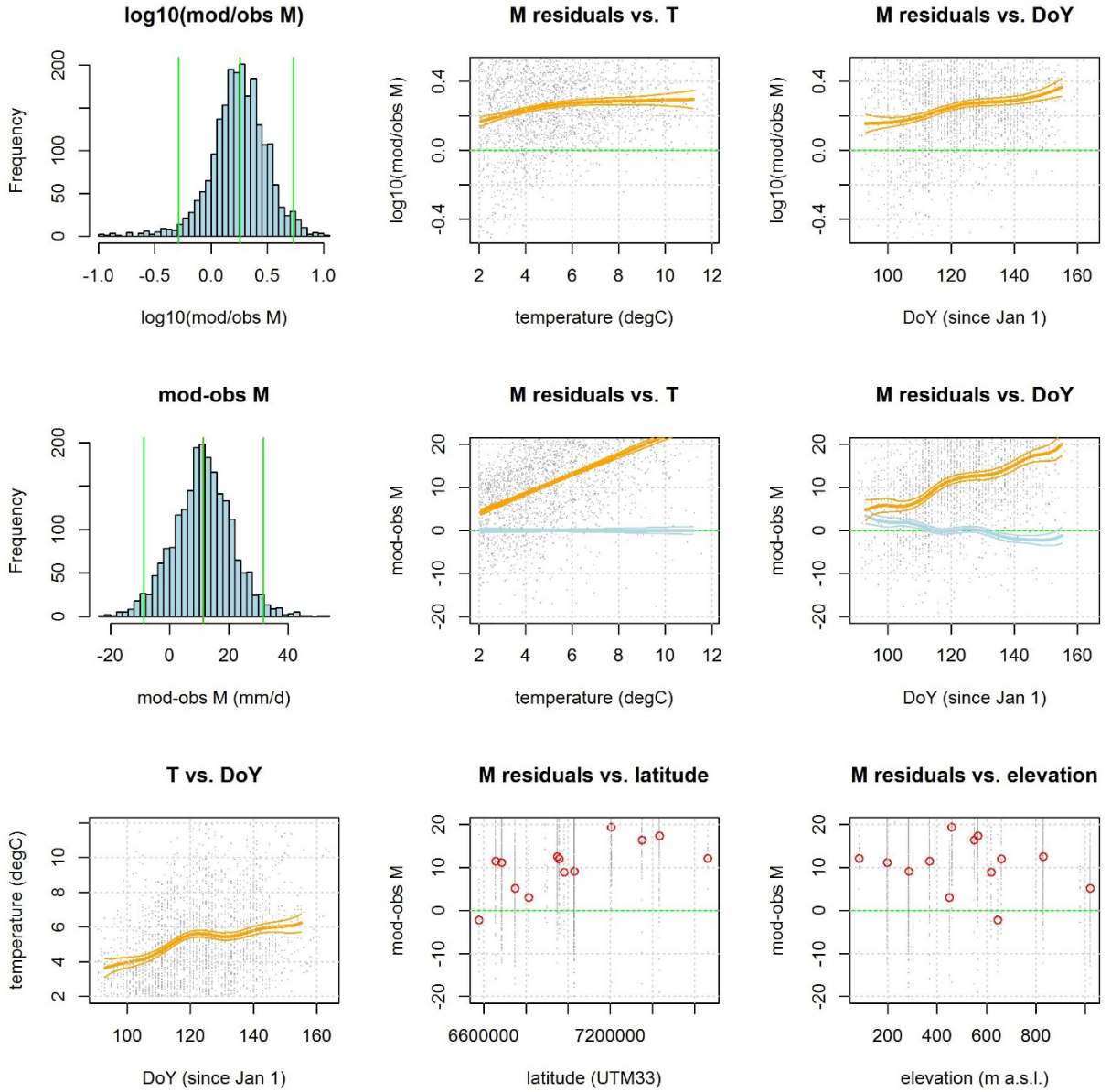


**Figure 8.** *seNorge\_EB* snow melt model fit and residuals for the forest subset of snow pillow data.

## 4 Discussion

### 4.1 Simulating accumulation and melt

From Table 1, it might appear that the *seNorge\_EB* model is superior to the degree day approach. According to the NS criterion 20 out of 31 stations are better modeled with the EB approach. Recall that the snow accumulation procedures are identical for all three tested accumulation-melt procedures (“EB” denotes the energy balance approach, “GD” the degree-day approach, and “SN” the operational *seNorge* model), they differ only in how snow melt is treated. In Figure 9 we find a comparison between the degree-day



approaches (GD and SN) and EB approach for the Filefjell site. The overall performance for all three models is very poor due to overestimated precipitation and underestimated temperature of the seNorge gridded data set, but the EB model comes out as less poor. In the figure a distinct difference in how snow is melted between the degree-day approaches and that of the EB model is seen, but which is the better one is difficult to tell.

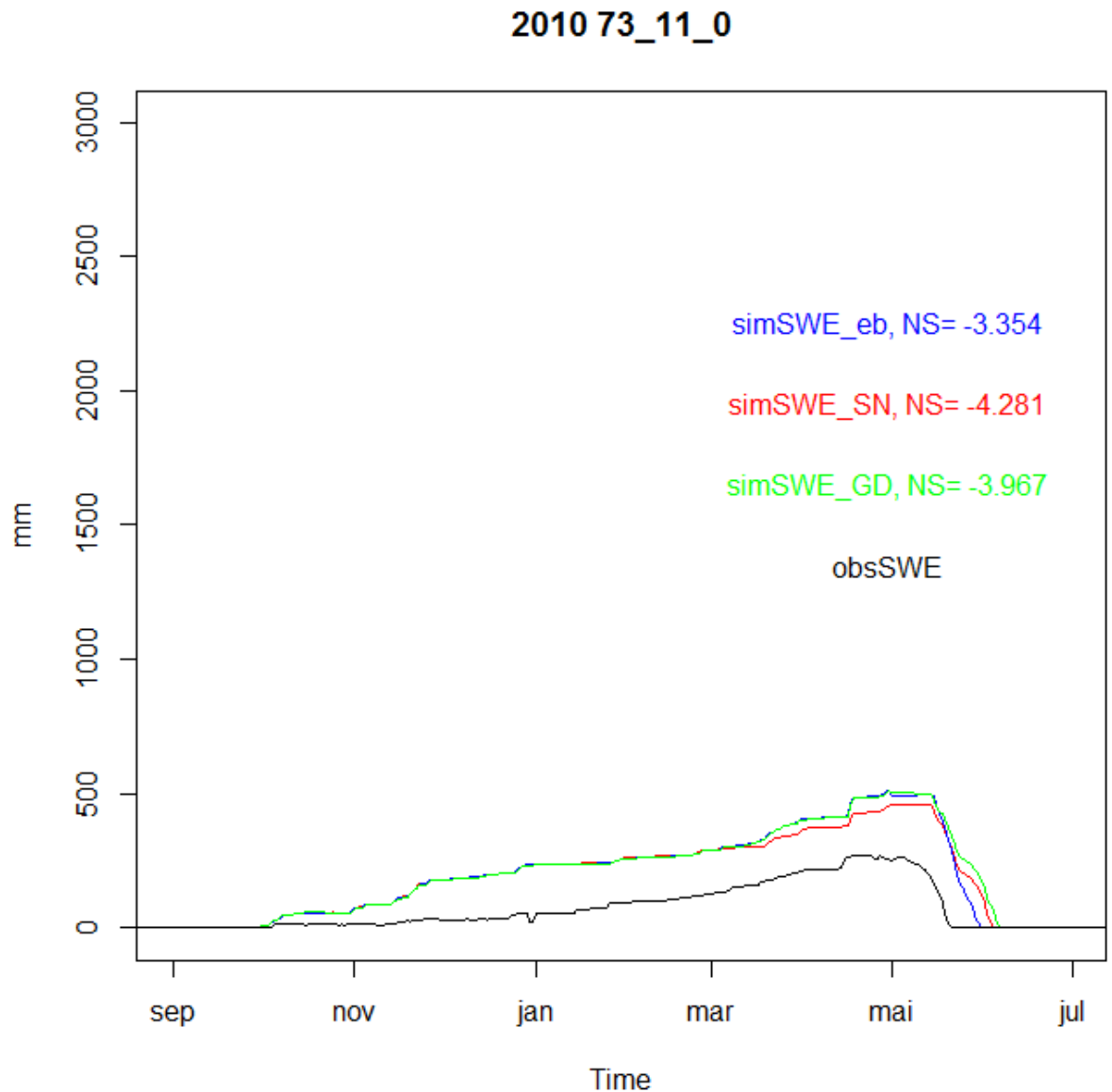


**Figure 9.** Simulated and observed simulation of SWE at the Filefjell research site. The Figure shows the difference in simulating SWE on a 24 hourly resolution using the degree-day model and the *seNorge\_EB* model.

Figure 10 shows the potential benefit of using an energy balance approach on a 3 hourly time step. The *seNorge\_EB* model is run with precipitation and temperature derived from the seNorge grid, but the 3 hourly input is disaggregated according to the procedure

described in Vormoor and Skaugen (2013). The two datasets of precipitation and temperature (24h and 3h) are consistent in that the daily sums are identical. The figure suggests that part of the bias problem of the seNorge data set also is a function of temporal resolution, but again, the apparently better timing of the 3 hourly model over the 24 hourly model might just be a function of different accumulations of the two models and not of superior simulated melt rates. This issue will be briefly discussed in the next sub-section.

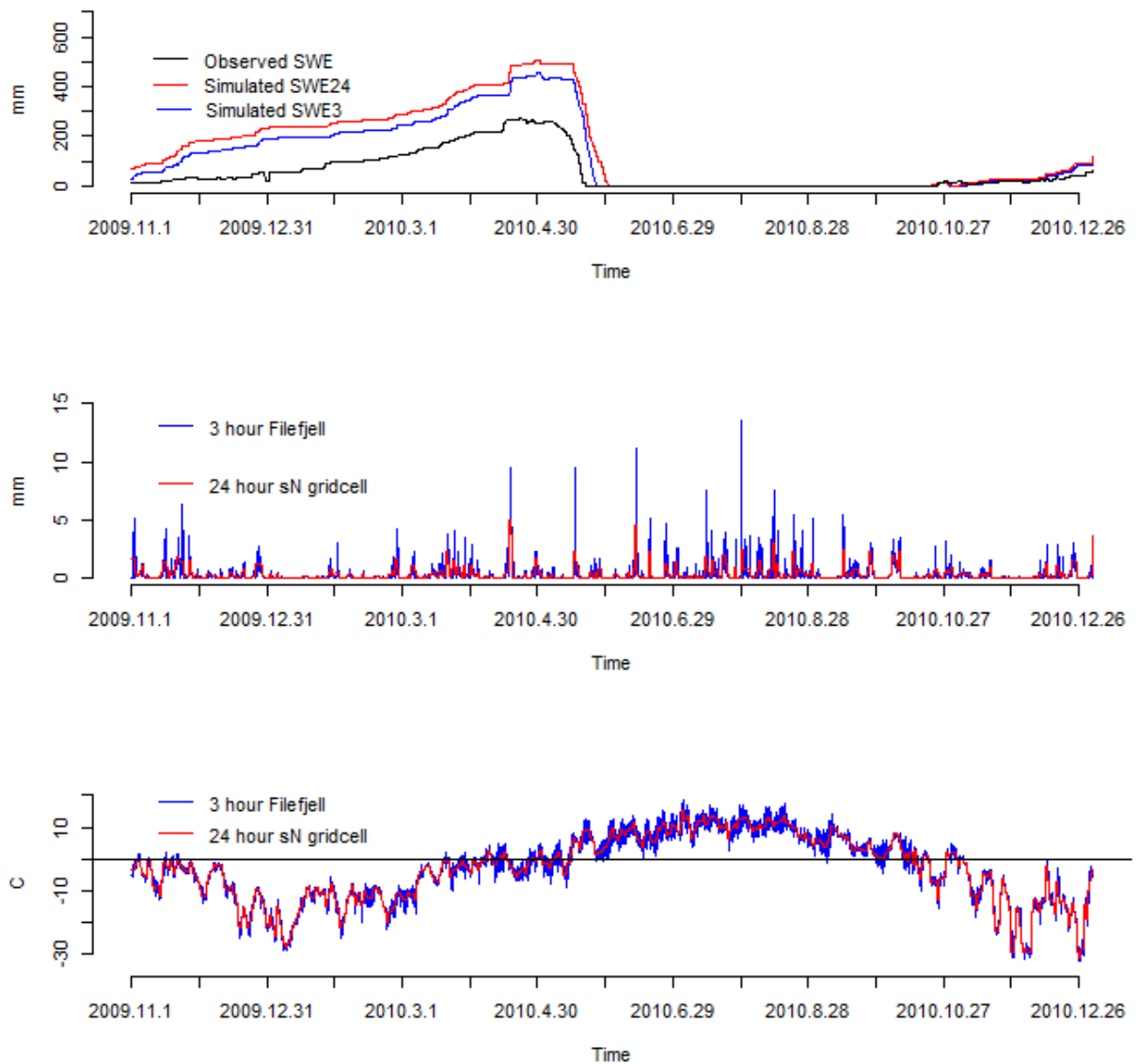


**Figure 10.** Simulated and observed simulation of SWE. The top panel shows the differences in simulating SWE with the *seNorge\_EB* model using 24 hourly and 3 hourly temporal resolution and the lower panels compare the input data for different temporal resolutions.

## 4.2 Simulating melt rates

From the results showed in section 3.2, is it clear that when only comparing simulated daily melt rates, the *seNorge\_EB* does not appear superior to the degree-day model, of *seNorge v.1.1.1*. There is a significant positive bias in the melt rates, and the discrepancy between observed and simulated melt rates increases with temperature (and daynumber of the year, which, of course, is highly correlated with temperature).

## 4.3 Future prospects

A sensitivity analysis of the *seNorge\_EB* model, where observed data such as incoming and outgoing short wave- and long wave radiation, wind speed and snow temperature is input to the model, will be carried out. The objective of such an analysis is to evaluate the weaknesses of the model and to reveal which elements of the energy balance is poorly simulated. In addition, there will be an assessment of which additional data to precipitation and temperature are strictly necessary in order to simulate snow melt rates with an acceptable precision for hydrological catchment modelling. At Filefjell snow research station such data is available as point values and a master student at UiO is currently conducting the analysis.

In addition, to increase model flexibility, an alternative solar radiation module for variable terrain topography, taking into account the elevation, slope and aspect of the site, is under development (see Allen et al. 2006).

The analysis presented here is not altogether complete in that *daily* melt rates are investigated for 31 snow pillows, whereas the *3-hourly* analysis is only carried out for Filefjell research station. It is at a sub-daily time step that an energy balance approach to snow melt, such as in *seNorge\_EB*, is expected to show its superiority.

The *seNorge\_EB* is considerably more complex than a simple degree-day approach to snow melt modelling, even though it has the possibility to run on precipitation and temperature as the only input data. The complexity of *seNorge\_EB* may very well represent an unsurmountable problem in that modelling at scales larger than point necessarily involves effective parameter values which may be difficult or impossible to estimate. Further analysis of the model will tell us of its sensitivities and hopefully suggest reasonable parameterisations of complex processes.

# Conclusions

The testing of an energy balance approach to snow melt modelling, only using precipitation- and temperature data as input, gave satisfactory results when we compared the simulated variables such as snow water equivalent (at 24 h), radiation and albedo (at 3h) to observed at 24- and 3 hourly time steps. However, the EB approach at daily resolution seemed to overestimate snow melt rates when compared to observed daily melt rates from the snow pillow stations. The obvious benefits of the EB approach are that 1) it is a more physically-based approach to snow melt modelling, and 2) the use of calibrated parameters (the degree-day parameter) can be avoided, especially since the dependence of solar radiation of location is implicitly taken into account.

# References

- Allen, R. G., Trezza, R. and Tasumi, M., 2006. Analytical integrated functions for daily solar radiation on slopes, *Agricultural and Forest Meteorology* 139, 55-73.
- Bacellar, S., Oliveira, A.P., Soares, J. and Servain, J., 2008. Assessing the diurnal evolution of surface radiation balance over the western region of Tropical Atlantic Ocean using in situ measurements carried out during the FluTuA Project. *Meteorol. Appl.* (doi: 10.1002/met)
- Campbell, G.S. and Norman, J.M., 1998. *An introduction to Environmental Biophysics*. Second ed., Springer New York. p.286.
- Dickinson, R. E., Henderson-Sellers and P. J. Kennedy, 1993. Biosphere-Atmosphere Transfer Scheme (BATS) version 1e as Coupled to NCAR Community Climate Model, NCAR/TN-387+STR, National Center for Atmospheric Research.
- Dingman, S. L., 2002. *Physical hydrology*. Second Ed. Prentice Hall, New Jersey. U.S.
- Goodison, B.E., Ferguson, H.L., McKay, G.A., 1981. Measurement and data analysis. In Gray, D.M., Male, D.H. (Eds.), *Handbook of Snow*, Pergamon Press, Toronto, ON, pp 191-274.
- Liston, G.E. 1995. Local advection of momentum, heat and moisture during melt of patchy snow covers. . *J. Appl. Meteorolgy*, **34** 1705-1715.
- Liston, G.E and K. Elder. 2006. A meteorological distribution system for high- resolution terrestrial modeling (MicroMet). *J. Hydrometeorology*, **7**(2), 217–234.
- Pielke Sr., R.A., G.E. Liston, W.L. Chapman and D.A. Robinson, 2004. Actual and insolation-weighted Northern hemisphere snow cover and sea-ice between 1973-2002. *Climate Dynamics*, 22,591-595 (doi:10.1007/s00382-004-0401-5).

Saloranta, T. M. 2014. New version (v.1.1.1) of the seNorge snow model and snow maps for Norway, *Rapport 6-2014, Norwegian Water Resources and Energy Directorate*, Oslo, Norway, 30 pp., available at:

[http://webby.nve.no/publikasjoner/rapport/2014/rapport2014\\_06.pdf](http://webby.nve.no/publikasjoner/rapport/2014/rapport2014_06.pdf)

Tarboton, D.G and C.H. Luce 1996. Utah energy Balance Snow Accumulation and Melt Model (UEB). Computermode and technical description and user guide.

Vormoor K. and T. Skaugen, 2014. Temporal disaggregation of daily temperature and precipitation grid data for Norway. *Journal of Hydrometeorology* (in press).

Walter, M.T., Brooks, E. S. McCool, D.K, King, L.G., Molnau, M. and Boll, J., 2005. Process-based snowmelt modeling: does it require more input data than temperature index modeling? *J. Hydrol.* **300**, 65-75.

Web page for calculating sun hours ([http://quantitative-ecology.blogspot.no/2007\\_10\\_01\\_archive.html](http://quantitative-ecology.blogspot.no/2007_10_01_archive.html))



Norges  
vassdrags- og  
energidirektorat

Norges vassdrags- og energidirektorat

Middelthunsgate 29  
Postboks 5091 Majorstuen  
0301 Oslo

Telefon: 09575  
Internett: [www.nve.no](http://www.nve.no)